The Astrophysical Journal, 525:995–1008, 1999 November 10

PROPERTIES OF HOT WHITE DWARFS IN EXTREME-ULTRAVIOLET/SOFT X-RAY SURVEYS[1]

Stéphane Vennes[2]
Department of Mathematics and Astrophysical Theory Centre, Australian National University, Canberra, ACT 0200, Australia; vennes@maths.anu.edu.au
Received 1999 May 6; accepted 1999 July 2

ABSTRACT

Intermediate-dispersion spectroscopy ($\Delta \sim 6$ Å) of 38 ultrasoft X-ray sources (*ROSAT* PSPC/WFC and *EUVE*)—27 H-rich white dwarfs (DA), one magnetic white dwarf (DAp), eight active galactic nuclei, a new cataclysmic variable, and an active late-type star—is presented. Atmospheric ($T_{\rm eff}$, log g) and stellar (age, mass) parameters of the DA white dwarfs are determined, for the first time in the case of 12 objects. Adding the present sample to the EUV-selected sample of previous studies by Vennes et al., I define an enlarged population of 141 hot white dwarfs and redetermine the DA white dwarf mass distribution taking into account improved mass measurements for ultramassive white dwarfs. High-dispersion spectroscopy ($\Delta \sim 1.0$–1.4 Å) of the Hα line core in a representative collection of white dwarfs (the ultramassive DA GD 50, two hot DAs, and the low-mass DA EUVE J0512−006) indicate low projected rotation velocity $v_{\rm rot}$ sin $i \leq 30$–65 km s^{-1} and no perceptible radial velocity variations in the low-mass white dwarf EUVE J0512−006. Questions on the origin and evolution of hot white dwarf stars are examined in light of these results.

Subject headings: stars: fundamental parameters — stars: magnetic fields — white dwarfs — X-rays: galaxies — X-rays: stars

1. INTRODUCTION

The population of young, EUV-selected, hydrogen-rich white dwarfs has been surveyed recently during the *ROSAT* WFC/PSPC and *Extreme Ultraviolet Explorer* (*EUVE*) missions, and their stellar properties have been investigated thoroughly (Vennes et al. 1997b; Marsh et al. 1997; Finley, Koester, & Basri 1997). From these studies, we concluded that the white dwarf mass distribution peaks near 0.58 $M_\odot$ (C cores without H envelopes) with a substantially larger population of ultramassive ($M \geq 1.1$ $M_\odot$) white dwarfs than previously known.

Low-mass white dwarfs ($M \leq 0.47$ $M_\odot$) and, at the other extreme, ultramassive white dwarfs ($M \geq 1.1$ $M_\odot$) may be the product of unusual evolutionary processes involving two close degenerate stars. Marsh, Dhillon, & Duck (1995) offered strong evidence that most of the low-mass white dwarfs in Bergeron, Saffer, & Liebert's (1992) optical survey are members of close double-degenerate stars, with the possible exception of WD 1614+136 and WD 1353+409. Maxted & Marsh (1998) also measured a low projected rotation velocity in these two objects, contradicting main theoretical expectations (Iben, Tutukov, & Yungelson 1997). Therefore, it appears that some low-mass white dwarfs are isolated. It was also suggested by Bergeron et al. (1992) that the ultramassive white dwarf GD 50 (~ 1.2 $M_\odot$) may be the result of the merger of two white dwarfs; a high rotation rate is expected (Segretain, Chabrier, & Mochkovitch 1997).

I present medium- and high-dispersion spectroscopy of a selection of hot white dwarfs obtained at the Anglo-Australian Observatory (AAO) and Mount Stromlo and Siding Spring Observatories (MSO, SSO). Medium-dispersion spectra (§ 2.2) support effective temperature and surface gravity measurements for 27 X-ray–selected (*ROSAT* PSPC) DA white dwarfs (§ 3.1) and contribute to a new sample of 141 EUV/soft X-ray–selected DAs (§ 4). High-dispersion spectra (§ 2.3) of four objects support radial and rotation velocity measurements, which allow us to test binary evolution scenarios (§ 3.2). I summarize in § 5. Finally, Appendix A describes the new magnetic cataclysmic variable 1RXS J1016.9−4103, and Appendix B describes the new active late-type star and galactic nuclei identifications among ultrasoft *ROSAT* PSPC sources.

2. OBSERVATIONS

2.1. *X-Ray Catalogs and Selection of the Candidates*

The photospheric layers of noninteracting white dwarfs with effective temperatures exceeding $\sim$25,000 K reach depths at which substantial EUV/soft X-ray emission occurs. EUV-selected catalogs of hot white dwarfs were compiled using the *EUVE*'s 100 Å (0.07–0.21 keV) and 200 Å (0.05–0.08 keV) bandpasses and *ROSAT*/WFC's S1 (0.09–0.21 keV) and S2 (0.06–0.11 keV) bandpasses (Pye et al. 1995; Kreysing et al. 1995; Bowyer et al. 1996; Lampton et al. 1997). Vennes et al. (1996, 1997b) studied the properties of 112 white dwarfs detected in the *EUVE* all-sky survey. Kreysing et al. (1995) and Lampton et al. (1997) provide lists of *ROSAT* all-sky survey counterparts to EUV detections, and Fleming et al. (1996) provide a partial catalog of *ROSAT* detections of white dwarf stars.

I primarily relied on the catalog of *ROSAT* all-sky survey sources (1RXS) presented by Voges et al. (1999),[3] restricting the search to HR1 ≤ -0.9 such that HR1 $\leq -1 + 3\Delta$HR1, where HR1 $\pm$ ΔHR1 is the hardness ratio defined over the A (0.1–0.4 keV) and B (0.4–2.0) bands, such that HR1 $= (B-A)(B+A)^{-1}$. The *ROSAT* all-sky survey catalog lists sources with count rates generally exceeding $\sim$0.05 counts s^{-1}. I augmented the sample with fainter sources drawn from the *ROSAT* pointed source catalog

[1] Based on observations obtained at the Mount Stromlo Observatory 74 inch telescope, the Siding Spring Observatory 2.3 m telescope, and the Anglo-Australian Observatory 4 m telescope.

[2] QE II Fellow of the Australian Research Council. Also Visiting Fellow at Mount Stromlo and Siding Spring Observatories.

[3] Voges et al. 1999 is the print version of the sky survey results that also can be accessed at www.rosat.mpe-garching.mpg.de/survey/rass-bsc/.

(1RXP, Voges et al. 1999; XUV, Kreysing et al. 1995), the joint *ROSAT* PSPC-*EUVE* catalog (*EUVE*, Lampton et al. 1997), and from a catalog of *ROSAT* PSPC white dwarf detections (RX, Fleming et al. 1996). Three ultramassive white dwarfs studied by Vennes et al. (1996, 1997b) were also observed. Table 1 lists the sample of X-ray–selected white dwarfs with spectroscopic follow-up observations. Twelve objects also have optical identifications (e.g., Palomar-Green, Hamburg-Schmidt, or Kiso surveys), which in some cases prompted a pointed observation (1RXP), and eight objects also have EUV detections (*ROSAT* WFC or *EUVE*). Only eight objects are without alternate catalog memberships, and a total of 12 objects were still without unequivocal spectroscopic identifications. In Appendices A and B, I present a cataclysmic variable (CV), and active galactic nuclei (AGN) and late-type star identifications found among the 1RXS ultrasoft source list.

2.2. *Medium-Dispersion Spectroscopy* (*MSO*, *SSO*)

The program of spectroscopic observations of X-ray–selected white dwarfs was initiated on 1997 April 1–3 with the 74 inch telescope at the MSO followed by observing runs with the same instrumentation on 1997 October 1–6, November 28–December 3, 1998 February 26–March 3, October 13–19, November 15–19, and 1999 April 9–11. Additional spectra were obtained with the 2.3 m telescope at SSO on 1998 January 19–24, 1998 May 26–31, and 1998 June 17–22. The set-up at MSO consisted of a Cassegrain spectrograph equipped with a 300 line mm^{-1} grating and a SITe 1752 × 532 CCD binned 2 × 2, resulting in a wavelength dispersion of 2.75 Å $pixel^{-1}$. The set-up at SSO consisted of the Double Beam Spectrograph (DBS) mounted at the Nasmyth focus and equipped with a 316 line mm^{-1} grating on the red side, a 300 line mm^{-1} grating on the blue side, and two SITe 1752 × 532 CCDs. The resulting wavelength dispersion is 2.08 Å $pixel^{-1}$ on the red side and 2.18 Å $pixel^{-1}$ on the blue side. The wavelength scale was established with FeAr arcs for the blue spectra and NeAr arcs for the red spectra, and the slit width was set to 2″ on both spectrographs (MSO and SSO). The spectral resolution is ∼6 Å. Figure 1 presents observations of the 27 X-ray–selected white dwarfs, and Figure 2 presents new observations of three ultramassive white dwarfs. Figure 3 shows red and blue spectra of the composite DAp plus K V star RX J0616.8−6457.

2.3. *High-Dispersion Spectroscopy* (*AAT*, *SSO*)

On 1997 November 24 and 25, I obtained high-dispersion spectra of Hα in the ultramassive white dwarfs GD 50, EUVE J0443−037, and EUVE J0653−564, as well as in

TABLE 1

SAMPLE OF 28 X-RAY–SELECTED WHITE DWARFS

Name[a]	R.A. (2000)	Decl. (2000)	m_V	Other Name	References
1RXP J0000.1+2956......	00 00 07.3	+29 57 00	15.1[b]	PG 2357+296	1
1RXS J0039.9+3132......	00 39 52.1	+31 32 30	14.66	GD 8	2
1RXS J0055.9−5114......	00 55 56.7	−51 13 55	17.1[b]	JL 217	3
RX J0104.7+0949.........	01 04 41.4	+09 49 41	14.46	PG 0102+096	1
1RXS J0205.8−1338......	02 05 49.0	−13 38 28	15.5[b]	GD 1104	4
XUV J0335.6−3450......	03 35 33.7	−34 50 01	16.0[b]	...	
1RXS J0337.2−4155......	03 37 15.0	−41 55 25	16.3[b]	EUVE	5
RX J0354.6+0508.........	03 54 40.2	+05 08 46	16.2	KUV 03520+0500	6
1RXP J0415.6−1140......	04 15 35.7	−11 40 28	17.6[b]	...	
1RXS J0415.7−4022......	04 15 39.8	−40 22 33	16.8[b]	RE	7
1RXP J0428.6+1658......	04 28 39.3	+16 58 12	13.92	EG 37, RE	8
1RXP J0443.8−7851......	04 43 46.9	−78 51 50	13.47	BPM 3523	9
1RXS J0445.8−3855......	04 45 50.8	−38 55 39	16.6[b]	...	
1RXS J0505.7+0158......	05 05 39.2	+01 58 29	15.3[b]	HS 0503+0154	10
1RXS J0557.0−1635......	05 57 01.3	−16 35 12	18.2[b]	...	
RX J0616.8−6457.........	06 16 51.8	−64 57 34	18.5[b]	RE	7
1RXS J0619.1−0828......	06 19 06.9	−08 28 07	15.5[b]	...	
1RXS J0800.4−4746......	08 00 23.9	−47 46 03 [S]	17.7[b]	...	
1RXS J0823.6−2525......	08 23 34.6	−25 25 15	16.4[b]	EUVE, RE	5, 7
1RXS J0959.6−2604......	09 59 37.3	−26 04 27	16.4[b]	...	
1RXS J1024.7−3021......	10 24 44.2	−30 21 00	16.0[b]	EUVE, RE	5, 7
1RXS J1200.9−3630......	12 00 55.4	−36 30 05	15.4[b]	EUVE	5
1RXS J1406.1−0758......	14 06 04.8	−07 58 30	15.82	PG 1403−077	1
1RXP J1417.7+1302......	14 17 40.2	+13 01 48	15.39	Feige 93	11
1RXS J1614.3−0833......	16 14 19.1	−08 33 27	14.3[b]	...	
1RXS J2034.9−2734......	20 34 54.7	−27 34 50	15.5[b]	...	
1RXS J2101.2+0835......	21 01 13.3	+08 35 09	15.1[b]	HS 2058+0823	10
RX J2207.7+2520.........	22 07 45.1	+25 20 21	14.47	EUVE, RE	5, 7

NOTE.—Units of right ascension are hours, minutes, and seconds, and units of declination are degrees, arcminutes, and arcseconds.

[a] Soft X-ray catalogs: 1RXS, 1RXP = Voges et al. 1999; XUV = Kreysing et al. 1995; *EUVE* = Lampton et al. 1997; RX J = Fleming et al. 1996.

[b] Magnitude estimated from our spectroscopy. Other magnitudes from Cheselka et al. 1993 and Schwartz et al. 1995.

REFERENCES.—(1) Green, Schmidt, & Liebert 1986; (2) Giclas et al. 1965; (3) Jaidee & Lynga 1969; (4) Giclas et al. 1975; (5) Bowyer et al. 1996; (6) Wegner & Boley 1993; (7) Pye et al. 1995; (8) Eggen & Greenstein 1965; (9) Luyten & Smith 1958; (10) Homeier et al. 1998; (11) Feige 1958.

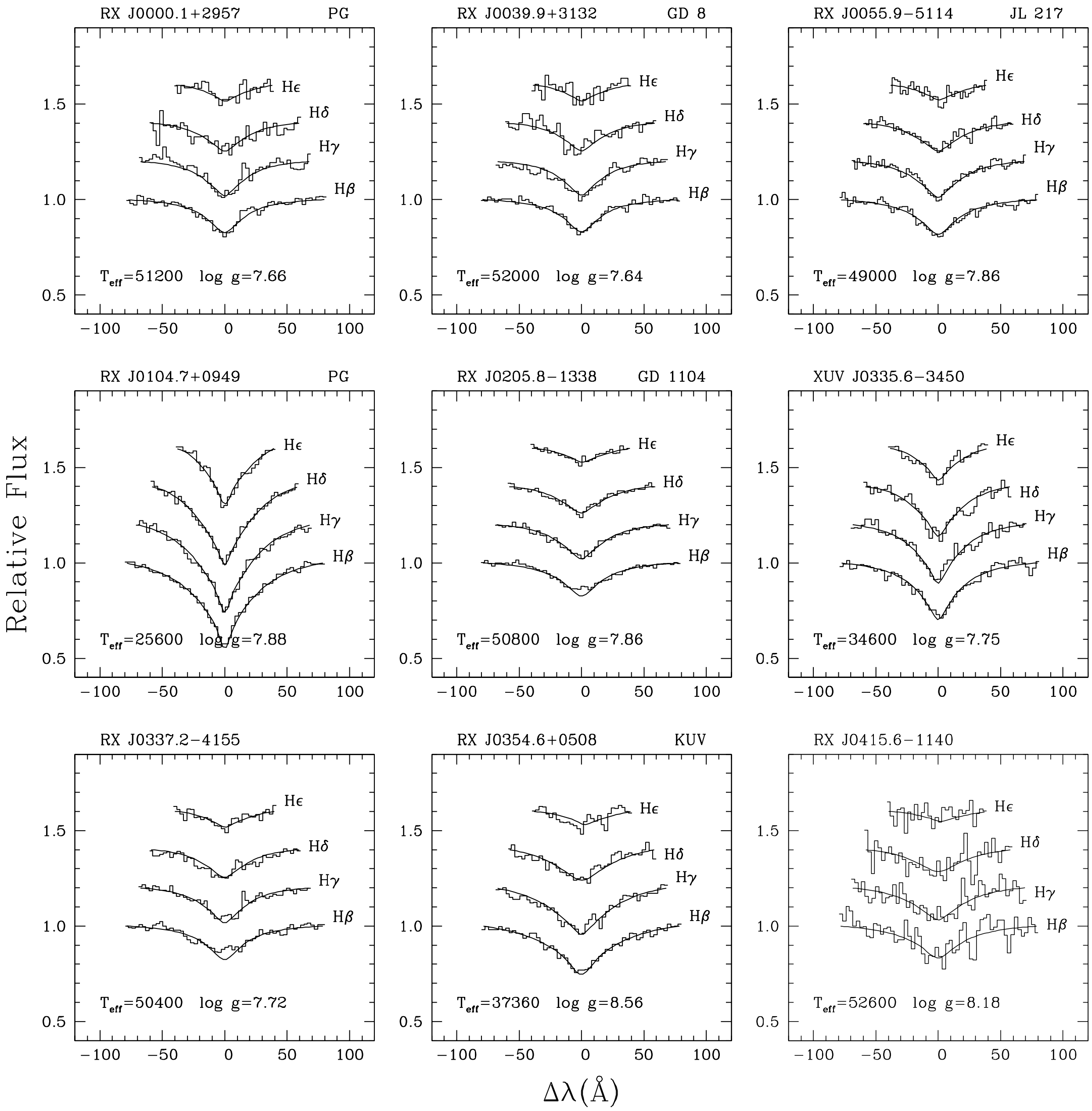

FIG. 1.—Model atmosphere fits to Balmer line spectra from 27 X-ray–selected white dwarfs. Note the relatively cool white dwarf 1RXP J0443.8 − 7851 (BPM 3523), the very hot DA 1RXS J0619.1 − 0828, and the low-mass white dwarf 1RXS J1417.7 + 1302 (Feige 93). Ferrario et al. (1998) presented a study of the ultramassive magnetic DA 1RXS J0823.6 − 2525.

the low-mass DA white dwarf EUVE J0512−006. I used the 4 m Anglo-Australian telescope (AAT) at the AAO and the Royal Greenwich Observatory (RGO) spectrograph equipped with a 1200 line mm^{-1} grating and a MIT 2048 × 4096 CCD resulting in a dispersion of 0.495 Å $pixel^{-1}$. The slit width was adjusted to 1''.4, and the resulting spectral resolution is 1.4 Å. I also obtained spectra of the radial velocity standard HR 3694 on both nights and established a velocity accuracy of $\Delta v \sim 4$ km s^{-1}. Detection of a narrow core was made only in the cases of GD 50 and EUVE J0512−006.

High-dispersion spectra of the bright DA white dwarfs EUVE J0623−376 and EUVE J2214−493 were obtained on 1998 May 28 with the 2.3 m telescope at the SSO. I used the DBS equipped with 1200 line mm^{-1} gratings on the blue and red sides, resulting in dispersions of 0.555 Å $pixel^{-1}$ and 0.548 Å $pixel^{-1}$ on the blue and red sides, respectively. I adjusted the slit width to 2'' for a spectral resolution of 1.0 Å. Figure 4 (*left-hand panel*) presents the normalized spectra, uncorrected for telluric absorption, and (*right-hand panel*) the corrected spectra.

3. A SAMPLE OF X-RAY–SELECTED WHITE DWARFS

3.1. *Effective Temperatures and Surface Gravities*

I first determine the effective temperature and surface gravity of the 27 X-ray–selected DA white dwarfs (Fig. 1, Table 2) and redetermine these parameters for three ultramassive white dwarfs (Fig. 2). I adopted the same methodology described in our previous work: synthetic Balmer line

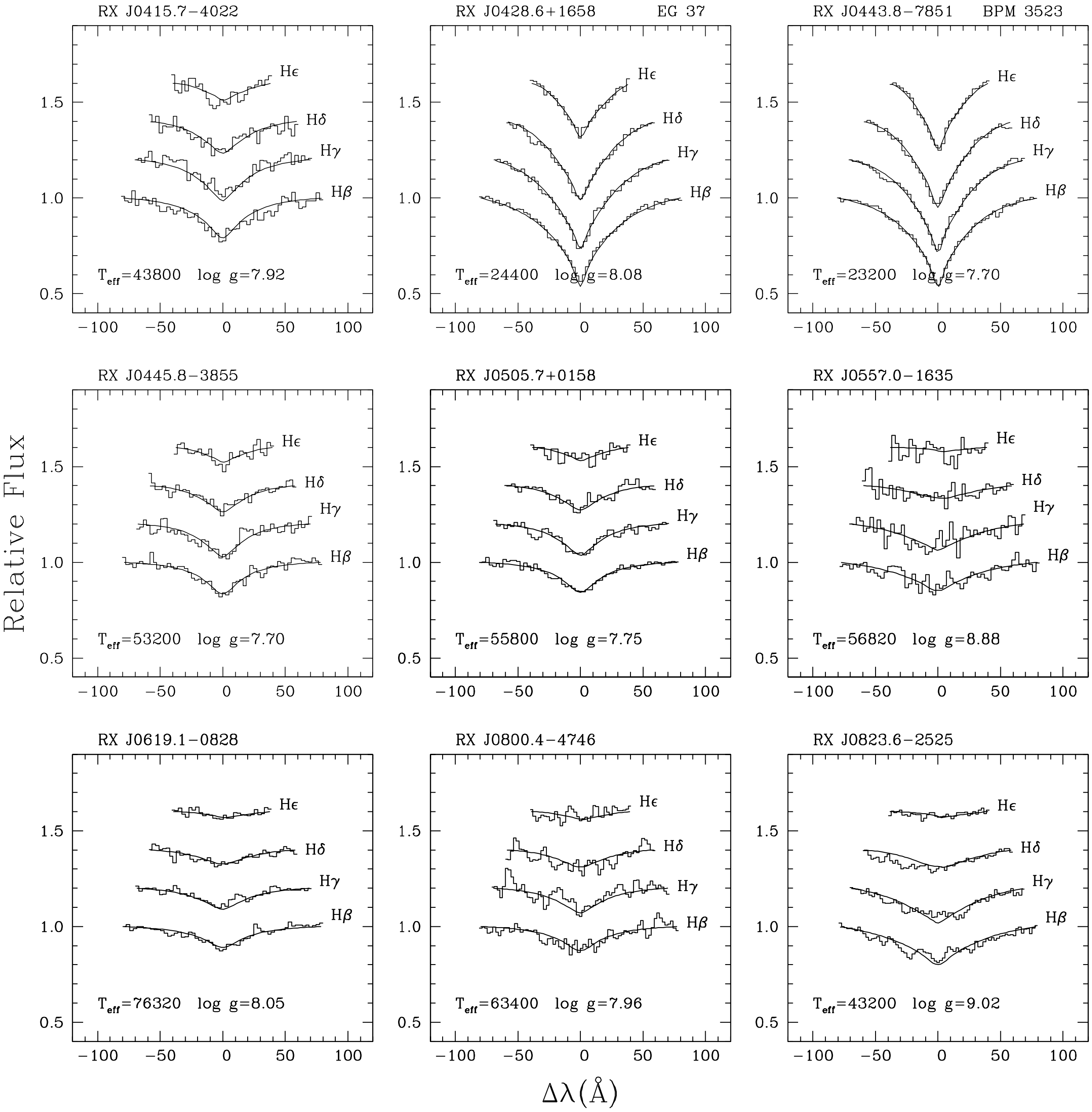

FIG. 1.—*Continued*

spectra are based on Stark-broadened line profiles (T. Schöning & K. Butler 1995, private communication) and a grid of LTE line-blanketed model atmospheres used in our earlier analysis of EUV-selected white dwarfs (Vennes et al. 1996, 1997a, 1997b), and best fits are obtained with χ^2 minimization techniques. Likely parameters for the magnetic white dwarf RX J0616.8−6457 are given in Figure 3, but a formal analysis awaits additional data. I now present a few notes on individual objects.

1RXP J0443.8−7851.— At $T_{eff} = 23{,}200$ K, the DA white dwarf BPM 3523 is among the coolest member of its class detected in EUV/soft X-ray surveys. Similar detections are CD $-38°10980$ at $T_{eff} = 24{,}700$ K (Vennes et al. 1996), EUVE J0902−041 at $T_{eff} = 24{,}200$ K (Vennes et al. 1997b), and, from the present sample, 1RXP J0428.6+1658 (= EG 37, VR 16) at $T_{eff} = 24{,}400$ K. The star EG 37 was among the coolest white dwarfs detected with *EXOSAT* pointed observations (see a discussion in Kidder et al. 1992). *ROSAT* PSPC pointed observations (Wolff, Jordan, & Koester 1996) reached even lower effective temperatures: GD 140 ($T_{eff} = 21{,}700$ K), GD 222 ($T_{eff} = 21{,}300$ K), and possibly Wolf 1346 ($T_{eff} = 21{,}000$ K). Enhanced EUV emission observed from cool white dwarfs constitutes a direct verification of the hydrogen line-blanketing/backwarming effect most effective in the high density of white dwarf atmospheres (see Wesemael et al. 1980).

1RXS J0505.7+0158.—The white dwarf was independently identified in the Hamburg-Schmidt survey (= HS 0503+0154) by Homeier et al. (1998), and their measured parameters are reported in Table 2. Wei et al. (1997) also report the identification of the white dwarf in optical follow-up spectroscopy of X-ray sources from PSPC pointed observations (= 1RXP J050540+0158.2) but did not measure stellar parameters.

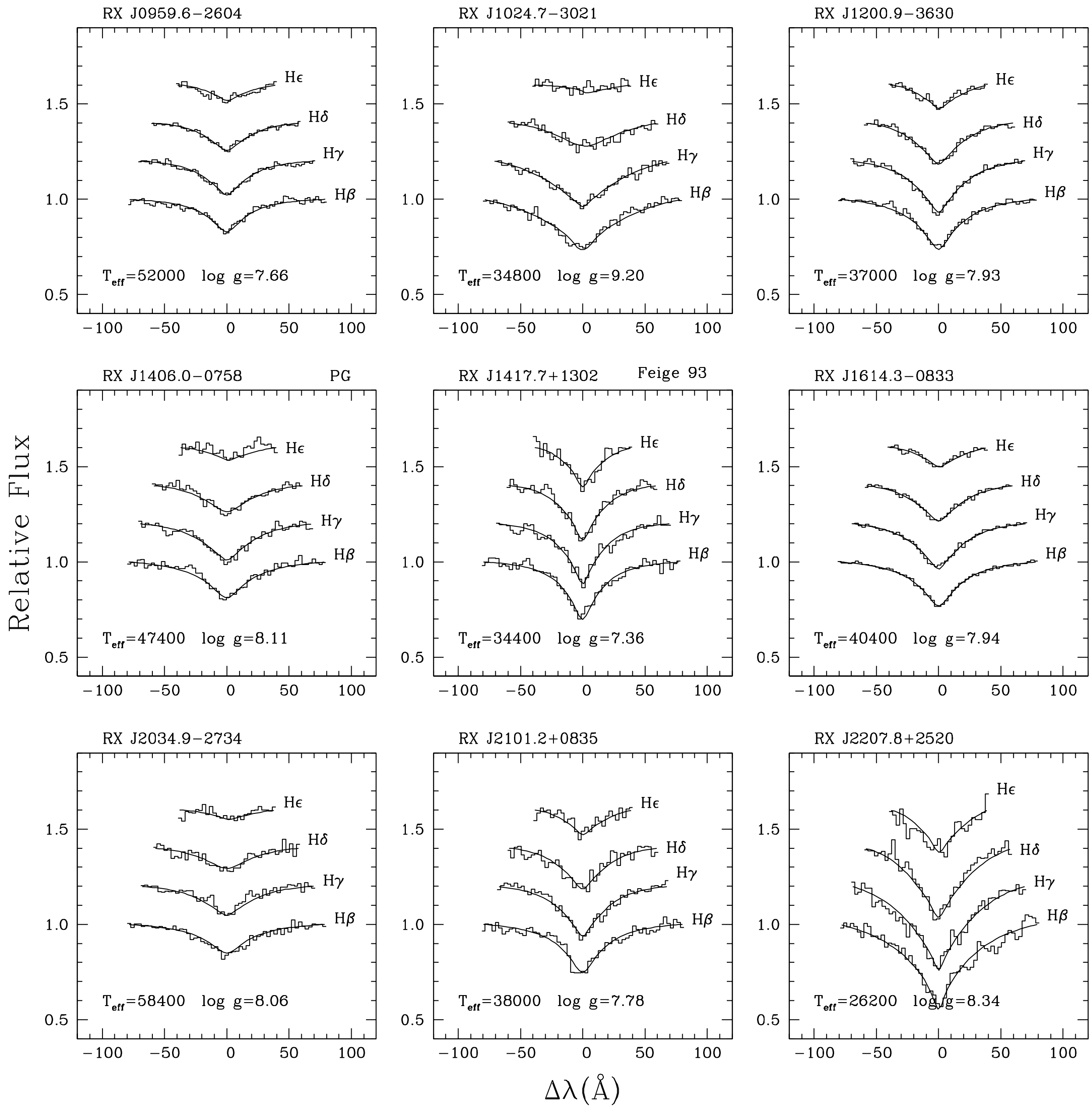

FIG. 1.—*Continued*

1RXS J0557.0−1635.—The faint ($V \sim 18$) optical counterpart to the X-ray source is possibly a new ultra-massive DA white dwarf, but additional spectra, with higher signal-to-noise ratios (S/N), are needed to improve the accuracy of the mass measurement.

RX J0616.8−6457.—The spectrum reveals a faint ($V = 18.5$) blue star near the X-ray source. Zeeman-displaced components of Hβ corresponding to an average field of $\langle B \rangle \sim$ 10–15 MG are tentatively identified. Figure 3 shows our spectrum along with a magnetic DA model, kindly provided by L. Ferrario, at $T_{\rm eff} = 50{,}000$ K, log $g = 8.0$, and $B_d = 14$ MG viewed at an inclination of 60°. Schmidt & Smith (1995) reported on the unpublished identification of RE J0616−645 by D. Finley and S. Jordan as a magnetic white dwarf.

1RXS J0619.1−0828.—This star is possibly one of the hottest hydrogen-rich white dwarfs detected in the *ROSAT* PSPC all-sky survey along with RE 1738+665 ($T_{\rm eff} \sim$ 90–95 $\times$ 10^3 K; Finley et al. 1997, Marsh et al. 1997). Some implications are a lower photospheric heavy-element abundance—making possible a high-energy detection—and, in general, the existence of a direct formation channel of hydrogen-rich white dwarfs alongside the helium/carbon-rich channel (PG 1159 stars and DO white dwarfs). Other extremely hot hydrogen-rich white dwarfs were also identified in the Hamburg-Schmidt Survey, such as HS 0615+6535 and HS 2246+0649 (both $T_{\rm eff} \sim 100{,}000$ K; Homeier et al. 1998).

1RXS J0800.4−4746.—The white dwarf is the southern counterpart of a close visual pair.

1RXS J0823.6−2525.—The EUV/soft X-ray source was wrongly identified with the bright F3 IV/V star HD 70907 in the *ROSAT* WFC and *EUVE* source catalogs. Ferrario et al. (1998) measured the dipolar magnetic field ($B = 3.5$

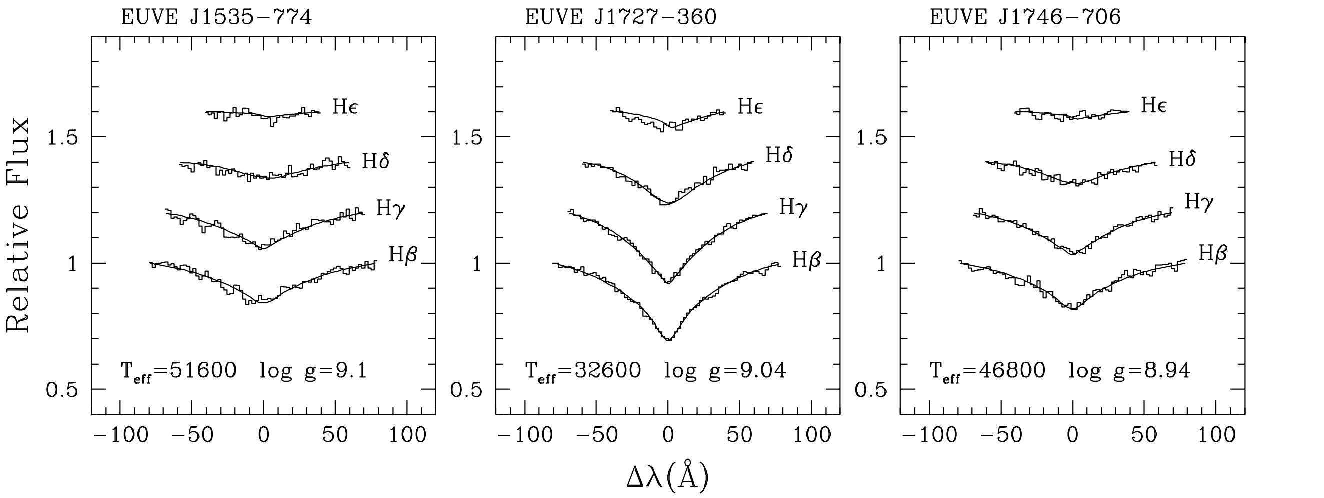

FIG. 2.—Atmospheric parameter determinations of three ultramassive white dwarfs. Although in agreement with earlier analyses, the new measurements supersede previous results in the mass-distribution calculation.

MG) of the white dwarf, which, combined with the high mass, reveals a striking similarity with the DAp white dwarf PG 1658+441 (Schmidt et al. 1992).

1RXS J1024.7−3021.—I confirm the high mass measured by Finley et al. (1997), thereby refuting the lower mass derived by Marsh et al. (1997). This massive white dwarf, along with the new massive white dwarf 1RXS J0557.0−1635, the isolated magnetic white dwarf 1RXS J0823.6−2525, and two magnetic white dwarfs in double-degenerate systems (EUVE J0317−855 and EUVE J1439+750), adds to a sample of 10 massive white dwarfs ($M \geq 1.2\ M_\odot$) studied by Vennes et al. (1997b).

1RXS J1417.7+1302.—Feige 93 is a low-mass white dwarf ($M \sim$0.36–0.41 $M_\odot$) that is also part of a spectroscopic binary (Greenstein 1986). Prominent Hα emission from the red dwarf companion (Finley et al. 1997) may be evidence of chromospheric activity or, most likely, of an EUV-irradiated chromosphere (see Thorstensen et al. 1978); variable Hα emission strength and velocity would indicate close proximity between the red dwarf and the hot EUV-emitting white dwarf. I present a radial velocity study of this object in § 3.2.

Both 1RXS J0205.8−1338 (GD 1104) and 1RXS J0337.2−4155 exhibit partly filled Hβ cores indicative of the presence of an unresolved low-mass main-sequence companion showing some level of activity.

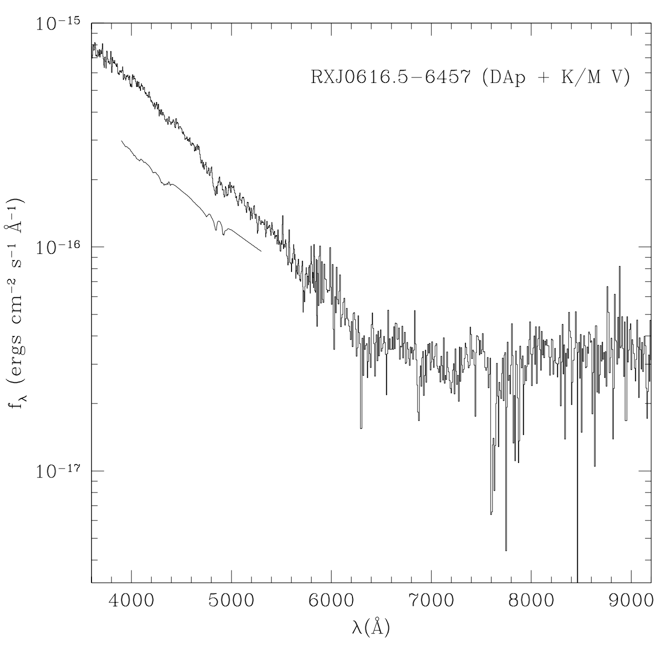

FIG. 3.—Red and blue spectra of the new magnetic white dwarf RX J0616.8−6457 along with a representative model at $T_{\rm eff}$ = 50,000 K, log g = 8 and B_d = 14.8 MG viewed at i = 60° (L. Ferrario 1998, private communication). Note evidence of a red companion (∼K V).

3.2. *Radial and Rotation Velocities*

The high-dispersion white dwarf spectra obtained at the AAT and at the SSO help constrain the projected rotation velocities of four white dwarfs (GD 50, EUVE J0512−006, EUVE J0623−376, and EUVE J2214−493), while the medium- and high-dispersion spectroscopic series of the known binary Feige 93 and suspected binary EUVE J0512−006 are examined for possible radial velocity variations. Based on Marsh et al.'s (1995) study of five low-mass DA white dwarfs in double degenerates, one would also expect the low-mass DA white dwarfs Feige 93 and EUVE J0512−006 to have emerged from close-binary evolution. Suggestions that ultramassive white dwarfs (such as GD 50) are the results of double-degenerate mergers (see Segretain et al. 1997) or that apparently isolated low-mass white dwarfs merged with their companions after the common envelope phase (Iben et al. 1997) would be verified with evidence of a high rotation rate. Alternatively, mechanisms responsible for efficient angular momentum loss—effectively erasing evidence of such mergers—are yet to be devised.

Radial velocities and full width half-maxima (FWHMs) of narrow emission features, such as Hα, have been measured using the Gaussian fitting function ("k") within IRAF's "splot" routine. A measurement of the FWHM Hα absorption/emission non-LTE (NLTE) core sets a useful upper limit to the white dwarf rotation velocity. The FWHM is related to the projected rotation velocity, $v \sin i$, by:

$$\frac{v \sin i}{c} = \frac{1}{\sqrt{3}} \frac{\sqrt{\mathrm{FWHM}^2 - \Delta^2}}{\lambda}\,, \tag{1}$$

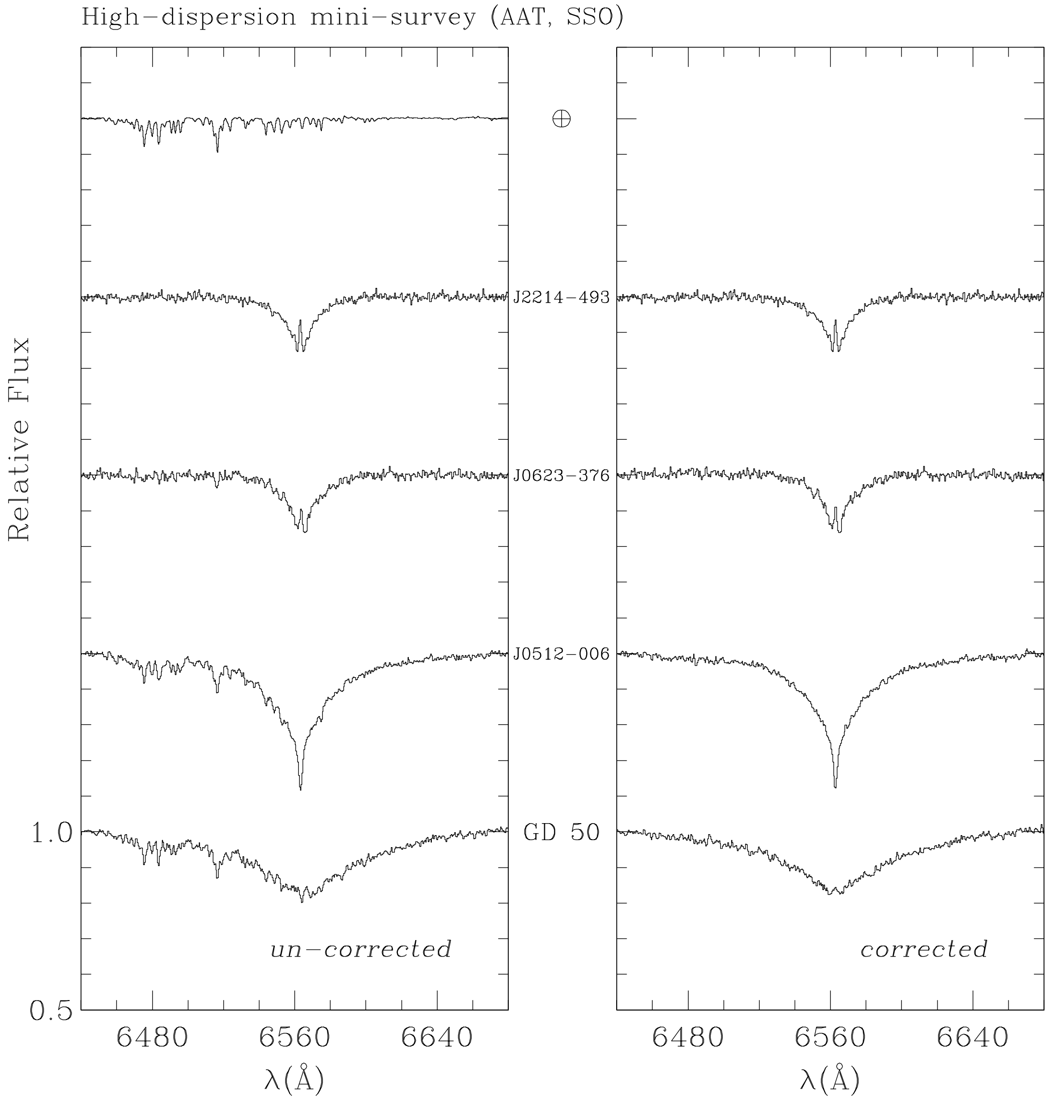

FIG. 4.—Minisurvey at AAO and SSO at resolution $\Delta = 1.0$–1.4 Å. *Left-hand panel*: Spectra uncorrected for telluric absorption. *Right-hand panel*: Spectra corrected following the relation $S_{\rm corr} = S \times T^{-n}$, where T is the telluric template (*top curve*) and n is a variable correction index ($n \sim 0$ for J2214−493, $n = 0.3$ for J0623−376, and $n = 1$ for J0512−006 and GD 50).

where Δ is the instrumental resolution ($\Delta \sim 1.0$ Å at SSO and ~ 1.4 Å at the AAT). Detailed line-profile calculations supplement this simple analysis: NLTE Hα line profiles were computed with TLUSTY (Hubeny 1988; Hubeny & Lanz 1995) adopting parameters from Vennes et al. (1997b). The profiles were convolved with a rotational broadening function and compared to data. A cross-correlation of spectral series may also be performed using IRAF's "fxcor" routine over prescribed wavelength ranges. Adopted techniques and results of these analyses are presented below for each star.

GD 50.—(Table 3, Fig. 5*a*) The first detection of a narrow NLTE Hα emission core in GD 50 establishes the feasibility of radial and rotation velocity studies in ultramassive white dwarfs. A series of six 1800 s exposures obtained at the AAT on 1997 November 24 and 25 shows no radial velocity variations and the summed spectrum reveals a narrow redshifted emission core at $+176$ km s^{-1}—compared with a predicted gravitational redshift of $+132$ km s^{-1} at log $g = 9$—and only 1.94 Å broad (FWHM). The rotation velocity measured from the FWHM (≤ 35 km s^{-1}) is comparable to an estimate based on the spectral synthesis (≤ 50 km s^{-1}). The analysis of the ground-state He II line series by Vennes et al. (1996), which suggested a large projected rotation velocity, is refuted and a high rotation rate, expected by theory (Segretain et al. 1997), is unlikely. The origin of ultramassive white dwarfs and the uncommon atmospheric H/He composition of GD 50 remain unexplained.

The line core shows no evidence of Zeeman splitting, which helps constrain the average magnetic field. A comparison of the Larmor frequency (eH/4π mc) with the Hα core half width at half-maximum (HWHM) limits the average field to $\leq 5 \times 10^4$ G, a limit consistent with Schmidt & Smith's (1995) spectropolarimetric study ($\leq 3 \times 10^4$ G).

EUVE J0512−006.—(Tables 3 and 4, Fig. 5*b*) Gaussian fits and cross-correlated velocities, using the narrow Hα absorption core in a series of nine spectra (900–1800 s) obtained at the AAT, limit potential radial velocity variations to 3–5 km s^{-1}. An upper limit to the rotation velocity, $v \sin i \leq 65$ km s^{-1}, is extracted from the mean spectrum, which is confirmed by a NLTE spectral synthesis. Note an

TABLE 2

EFFECTIVE TEMPERATURE AND SURFACE GRAVITY OF X-RAY–SELECTED WHITE DWARFS

	This Work				Other Work				
Identifier	T_{eff} (K)	ΔT_{eff} (K)	log g (cgs)	Δlog g (cgs)	T_{eff} (K)	ΔT_{eff} (K)	log g (cgs)	Δlog g (cgs)	References
0000.1+2956......	51200	1700	7.66	0.16	49939	695	7.60	0.06	1
0039.9+3132......	52000	2000	7.64	0.16	48900	240	7.85	0.02	2
					48655	520	7.74	0.05	1
0055.9−5114......	49000	1200	7.86	0.10	...	...	...	...	...
0104.7+0949......	25600	300	7.88	0.04	24495	117	7.87	0.02	1
0205.8−1338......	48600	1600	7.98	0.12	...	...	...	...	...
0335.6−3450......	34600	450	7.75	0.10	34848	600	7.95	0.05	3
0337.2−4155......	50000	1800	7.68	0.15	51737	4000	7.61	0.20	3
0354.6+0508......	37400	800	8.56	0.09	36400	170	8.85	0.04	2
0415.6−1140......	52600	3600	8.18	0.30	...	...	...	...	...
0415.7−4022......	43800	1300	7.92	0.18	...	...	...	...	...
0428.6+1658......	24400	300	8.08	0.04	23784	140	8.03	0.02	1
0443.8−7851......	23200	400	7.70	0.07	23614	78	7.83	0.04	4
0445.8−3855......	49200	2700	7.75	0.22	...	...	...	...	...
0505.7+0158......	55800	2500	7.75	0.20	57400	460	7.86	0.03	2
0557.0−1635......	56820	4500	8.88	0.24	...	...	...	...	...
0619.1−0828......	76320	200	8.05	0.15	...	...	...	...	...
0800.4−4746......	63400	2600	7.96	0.26	...	...	...	...	...
0823.6−2525......	43200	1000	9.02	0.10	...	...	...	...	...
0959.6−2604......	52000	1000	7.66	0.07	...	...	...	...	...
1024.7−3021......	34800	500	9.20	0.12	35733	196	8.95	0.03	1
					36610	$^{+1750}_{-830}$	8.69	$^{+0.11}_{-0.19}$	5
1200.9−3630......	37000	200	7.93	0.06	...	...	...	...	...
1406.1−0758......	47400	1000	8.11	0.10	49342	733	7.59	0.07	1
1417.7+1302......	34400	400	7.36	0.10	34400	140	7.31	0.03	6
					34004	105	7.43	0.02	1
1614.3−0833......	40400	300	7.94	0.05	38500	$^{+390}_{-340}$	7.85	$^{+0.05}_{-0.06}$	5
2034.9−2734......	58400	1800	8.06	0.14	...	...	...	...	...
2101.2+0835......	38000	600	7.78	0.11	36835	100	7.86	0.02	2
2207.7+2520......	26200	700	8.34	0.09	26559	141	8.30	0.02	1
					24610	$^{+80}_{-120}$	8.16	$^{+0.04}_{-0.02}$	5

REFERENCES.—(1) Finley, Koester, & Basri 1997; (2) Homeier et al. 1998; (3) Craig et al. 1997; (4) Bragaglia, Renzini, & Bergeron 1995; (5) Marsh et al. 1997; (6) Bergeron et al. 1994.

inconsistency between predicted line wings and the strength of the NLTE absorption core. Maxted & Marsh (1998) also measured a low rotation velocity in high-dispersion spectroscopy of two other low-mass DA white dwarfs.

EUVE J0623−376.—(Table 3, Fig. 5*c*) Reid & Wegner (1988) observed a narrow Hα emission core in the hot DA white dwarf G191-B2B that Vennes, Thejll, & Shipman (1991) later interpreted as an NLTE effect in hot white dwarfs. A similar detection in EUVE J0623−376 is compared with an NLTE model adopting parameters from Vennes et al. (1997b) fits to the upper Balmer line series. Note that Hα appears blueshifted relative to FUV heavy-element line velocities (Holberg, Barstow, & Sion 1998). Onset of the Balmer line problem is evident in Hβ and more so in Hα, an effect caused by heavy-element opacities (Werner 1996). A narrow Hα core limits the magnetic field to 3×10^4 G and the projected rotation velocity to 30 km s^{-1}. Wesemael, Henry, & Shipman (1984) obtained a similar limit to the rotation velocity of another hot DA white dwarf (Feige 24) based on FUV heavy element lines.

TABLE 3

AVERAGE RADIAL VELOCITY AND ROTATION VELOCITY

Name	$v_{H\alpha}$ (km s^{-1})	$v^{a}_{CNOSiFeNi}$ (km s^{-1})	$v \sin i$ (km s^{-1})
GD 50	+176.0 ± 6.0	...	≤35
EUVE J0512−006......	+23.6 ± 4.0	...	≤65
EUVE J0623−376......	+28.9 ± 4.0	+40.5 ± 0.5	≤30
EUVE J2214−493......	+31.1 ± 4.0	+33.9 ± 0.5	≤30

[a] Heavy-element line velocities from Holberg et al. 1998.

TABLE 4

RADIAL VELOCITY: EUVE J0512−006 SERIES

	v (km s^{-1})[a]	
HJD (2,450,000+)	Gaussian Fit	Cross-Correlation
777.0585...........	+22.4	+22.6
777.1773...........	+19.3	+20.4
778.0506...........	+33.3	+23.3
778.0638...........	+33.3	+27.1
778.0763...........	+20.0	+19.9
778.0888...........	+25.0	+20.8
778.1179...........	+19.9	+17.8
778.1311...........	+24.4	+24.7
778.1436...........	+26.7	+23.2

[a] Velocities measured with (1) Gaussian fits to narrow Hα line core and (2) cross-correlations against summed spectrum over $\lambda\lambda$6555–6570.

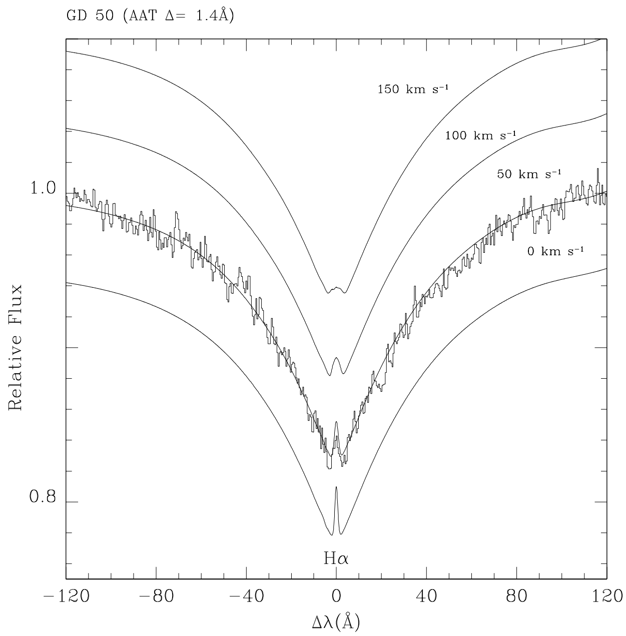

FIG. 5*a*

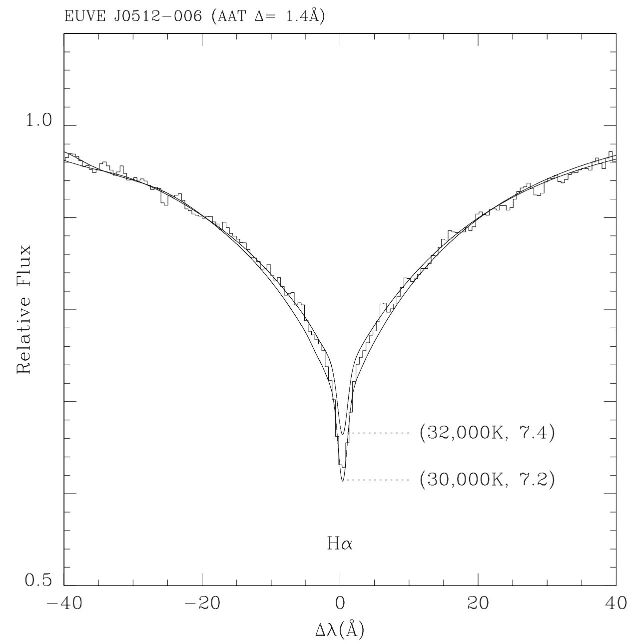

FIG. 5*b*

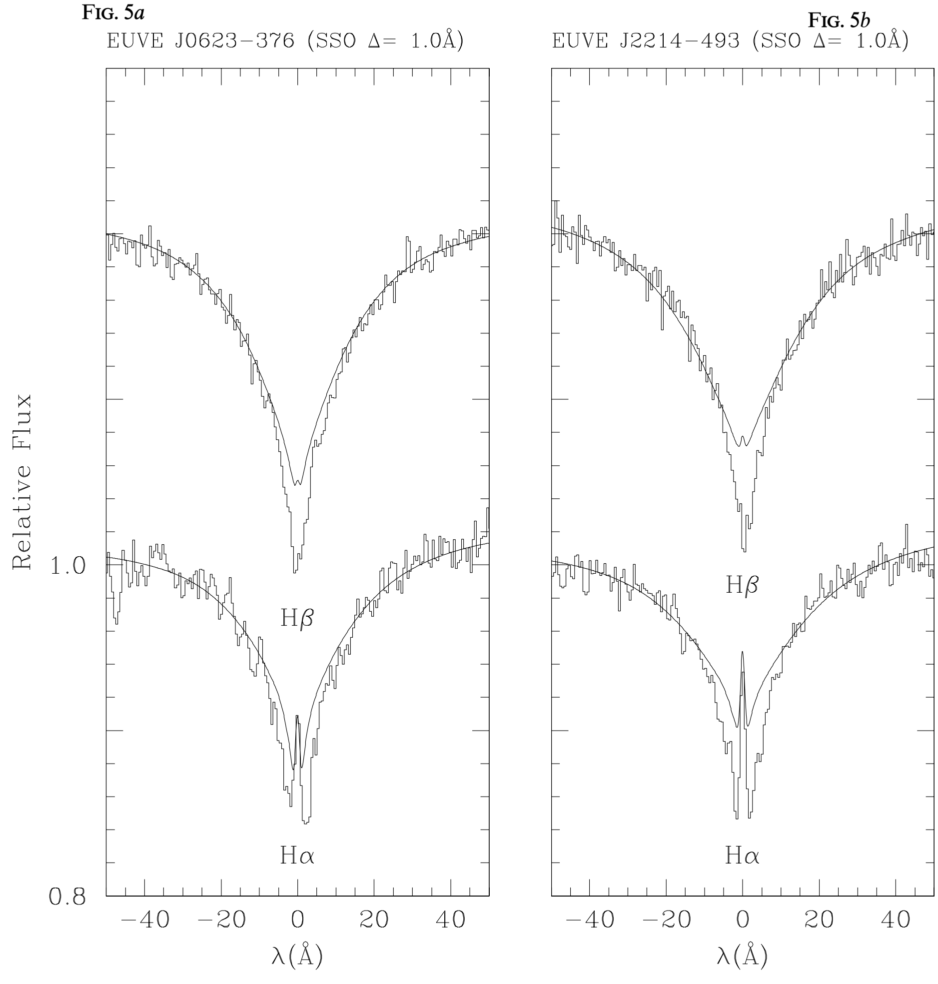

FIG. 5*c*

FIG. 5.—(*a*) Analysis of high-mass DA GD 50 with NLTE model at $T_{\rm eff} = 40{,}000$ K, $\log g = 9.0$ and $n({\rm He})/n({\rm H}) = 2.5 \times 10^{-4}$. Added rotation broadening ($v \sin i = 50, 100, 150$ km s^{-1}) to the model limits the rotation velocity $v \sin i \leq 50$ km s^{-1}. (*b*) Analysis of low-mass DA EUVE J0512−006 with two different pure-H NLTE models labeled with ($T_{\rm eff}$, $\log g$) and without rotation broadening. Note an inconsistency between fits to the line core and wings. (*c*) Analyses of ultrahot DA EUVE J0623−376 and EUVE J2214−493 with pure-H NLTE models adopting Vennes et al.'s (1997b) Balmer line fits: ($T_{\rm eff}$, $\log g$) = (64,000, 7.5) for J2214−493 and ($T_{\rm eff}$, $\log g$) = (62,000, 7.2) for J0623−376. Note evidence of the so-called Balmer line problem in both objects, presumably caused by heavy element opacities.

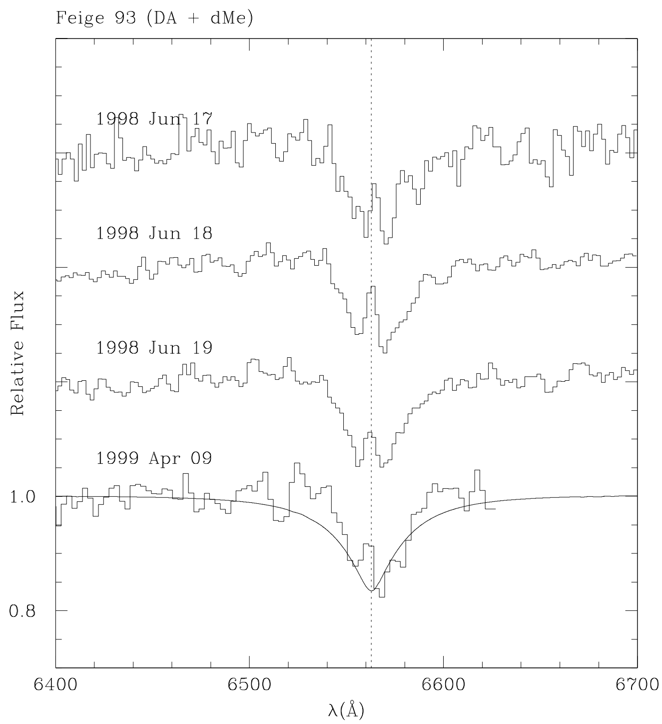

FIG. 6.—Hα spectroscopy (1998 June and 1999 May) showing possible radial velocity variations on a timescale of several days.

1RXS J1417.7+1302.—(Table 5, Fig. 6) Intermediate-dispersion spectra obtained at the 2.3 m telescope (SSO) on 1998 June 17, 18, and 19 and at the 74 inch (1.85 m) telescope (MSO) on 1999 April 9 show variations in Hα emission velocities but only modest variations in emission strength (EW $\sim 1.0 \pm 0.3$ Å). Cross-correlation of Hβ/Hγ spectra of the white dwarf may indicate radial velocity variations at the limit of detection ($K_{DA} \leq 25$ km s^{-1}). Strong Hα emission noted by Finley et al. (1997) largely exceeds our own equivalent width measurements, thus suggesting that the red dwarf may be flaring. High-dispersion data are required to resolve the dMe emission spectrum and the DA narrow absorption spectrum.

EUVE J2214−493.—(Table 3, Fig. 5*c*) A case similar to EUVE J0623−376, the high-dispersion spectrum also implies low rotation velocity and weak magnetic field. Contrary to EUVE J0623−376, the Hα velocity appears to be in good agreement with FUV heavy-element line velocities (Holberg et al. 1998). The low rotation velocities measured at AAT and SSO support the notion that, as a population, white dwarfs are slow rotators (see Heber, Napiwotzki, & Reid 1997, and references therein). The same conclusion extends to more exotic objects, such as the low-mass (see Maxted & Marsh 1998) and high-mass white dwarfs.

TABLE 5

RADIAL VELOCITY: FEIGE 93 SERIES

HJD (2,450,000+)	v (km s^{-1})[a]
982.03	+83.0 ± 25.0
982.98	+1.0 ± 25.0
983.91	−34.0 ± 25.0
1278.12	−51.0 ± 30.0

[a] dMe velocities measured with Gaussian fits to the Hα emission core.

4. MASS DISTRIBUTION

4.1. *Improved Mass Measurements*

The new mass distribution benefits from higher S/N spectroscopy and from the addition of Wood's (1995) evolutionary mass-radius relation at 1.2 $M_\odot$ (C interior, $10^{-5} M_*$ He envelope) and Hamada & Salpeter's (1961) C-interior relations at 1.3 and 1.35 $M_\odot$. Earlier measurements presented in Vennes et al. (1997b) extrapolated from the relation at 1.1 $M_\odot$, which resulted in inaccurate mass estimates at $M \geq 1.2\ M_\odot$. The present mass distribution is therefore considered definitive as far as our own effective temperature and surface gravity measurements are concerned, in particular at high masses. Table 6 presents mass measurements of the newly selected white dwarfs and Table 7 presents revised mass measurements for ultramassive white dwarfs ($M \geq 1.1\ M_\odot$).[4] White dwarfs with masses lower than 1.1 $M_\odot$ are not affected by the improved procedure.

4.2. *Overall Mass Distribution*

I have assembled 141 hot DA white dwarfs. I draw 18 objects from the southern, EUV-selected sample of Vennes et al. (1996), 92 objects from the EUV-selected sample of Vennes et al. (1997b), two other white dwarfs from Vennes et al. (1997a), and 27 objects from the present study, to

TABLE 6

MASS, ABSOLUTE LUMINOSITY, AND DISTANCE OF 29 X-RAY–SELECTED WHITE DWARFS

	CHe MODELS			
NAME	M ($M_\odot$)	ΔM ($M_\odot$)	M_V (mag)	d (pc)
1RXP J0000.1+2956	0.50	0.06	8.69	191
1RXS J0039.9+3132.......	0.50	0.06	8.62	161
1RXS J0055.9−5114.......	0.58	0.05	9.07	403
RX J0104.7+0949	0.54	0.02	10.20	71
1RXS J0205.8−1338.......	0.63	0.06	9.29	174
XUV J0335.6−3450	0.50	0.05	9.38	210
1RXS J0337.2−4155.......	0.51	0.06	8.74	325
RX J0354.6+0508	0.97	0.05	10.56	122
1RXS J0415.6−1140.......	0.75	0.18	9.52	413
1RXS J0415.7−4022.......	0.60	0.10	9.29	317
1RXS J0428.6+1658.......	0.65	0.02	10.58	46
1RXP J0443.8−7851	0.46	0.03	10.11	46
1RXS J0445.8−3855.......	0.53	0.10	8.89	348
1RXS J0505.7+0158.......	0.54	0.09	8.75	204
1RXS J0557.0−1635.......	1.15	0.09	10.75	309
1RXS J0619.1−0828.......	0.71	0.08	8.93	206
1RXS J0800.4−4746.......	0.65	0.14	8.96	559
1RXS J0823.6−2525.......	1.21	0.04	11.30	104
1RXS J0959.6−2604.......	0.50	0.03	8.67	351
1RXS J1024.7−3021.......	1.27	0.03	11.96	64
1RXS J1200.9−3630.......	0.59	0.03	9.54	148
1RXS J1406.1−0758.......	0.70	0.06	9.52	182
1RXP J1417.7+1302	0.36	0.03	8.78	210
1RXS J1614.3−0833.......	0.60	0.03	9.44	93
1RXS J2034.9−2734.......	0.69	0.08	9.22	180
EUVE J2055.5+1627......	0.85	0.03	10.20	104
1RXS J2101.2+0835.......	0.52	0.05	9.27	146
1RXS J2124.9+2825.......	0.48	0.01	8.50	100
RX J2207.7+2520	0.82	0.06	10.83	53

[4] Note that the white dwarf companion (EUVE J2126+193) to the A8V star HR 8210 is also an ultramassive white dwarf (see Landsman, Simon, & Bergeron 1993).

TABLE 7

EUV/Soft X-Ray Sample of Ultramassive White Dwarfs ($\geq 1.1\ M_\odot$)

Name	$T_{\rm eff}$ (K)	log g (cgs)	References	M ($M_\odot$)
EUVE J0003+435	42400 ± 1200	9.30 ± 0.12	1	1.30 ± 0.03
EUVE J0138+253	39400 ± 1200	9.12 ± 0.13	1	1.24 ± 0.04
EUVE J0317−855B[a,b]	30–50,000	9.3–9.6	2	1.33 ± 0.03
EUVE J0348−009	43200 ± 500	9.21 ± 0.05	1	1.27 ± 0.01
EUVE J0443−037	65140 ± 2600	9.12 ± 0.12	1	1.25 ± 0.03
1RXS J0557.0−1635........	56820 ± 4500	8.88 ± 0.24	3	1.15 ± 0.09
EUVE J0653−564	35200 ± 600	8.88 ± 0.10	1	1.14 ± 0.05
1RXS J0823.6−2525[a]	43200 ± 1000	9.02 ± 0.10	3	1.21 ± 0.04
EUVE J0916−197	56400 ± 2600	9.12 ± 0.20	1	1.25 ± 0.06
1RXS J1024.7−3021........	34800 ± 500	9.20 ± 0.12	3	1.27 ± 0.03
EUVE J1439+750B[a,b]	20–50,000	8.45–9.0	5	1.06 ± 0.14
EUVE J1535−774	51600 ± 1500	9.10 ± 0.10	3	1.24 ± 0.03
EUVE J1659+440[a]	30510 ± 200	9.36 ± 0.07	6	1.31 ± 0.02
EUVE J1727−360	32600 ± 200	9.04 ± 0.05	3, 7	1.21 ± 0.02
EUVE J1746−706	46800 ± 800	8.94 ± 0.08	3	1.18 ± 0.03

[a] Also a magnetic white dwarf.

[b] Also part of a double degenerate star.

References.—(1) Vennes et al. 1997b; (2) Ferrario et al. 1997; (3) this work; (4) Ferrario et al. 1998; (5) Vennes et al. 1999a; (6) Schmidt et al. 1992; (7) Dupuis & Vennes 1997.

which I add analyses of the magnetic white dwarfs in the double degenerates EUVE J0317−855 and EUVE J1439+750 (Ferrario et al. 1997; Vennes, Ferrario, & Wickramasinghe 1999a). I also updated the parameters of HZ 43 with the analysis of Dupuis et al. (1998). Figure 7 shows all measurements in the ($T_{\rm eff}$, log g) plane (*top panel*) and the (age, mass) plane (*bottom panel*). Note that ultramassive white dwarfs selected in EUV/soft X-ray surveys are possibly some 10 times older than their lower mass counterparts with similar effective temperatures—hence similar detection probabilities—which implies a considerably smaller birthrate.

The presence of so many ultramassive objects in EUV/soft X-ray surveys may therefore correspond to an evolutionary bottleneck occurring early on during the cooling sequence and naturally covered by these surveys.

Figure 8 presents the new mass distribution based on the EUV/soft X-ray sample of 141 objects. The distribution shows four peaks corresponding to population growths at

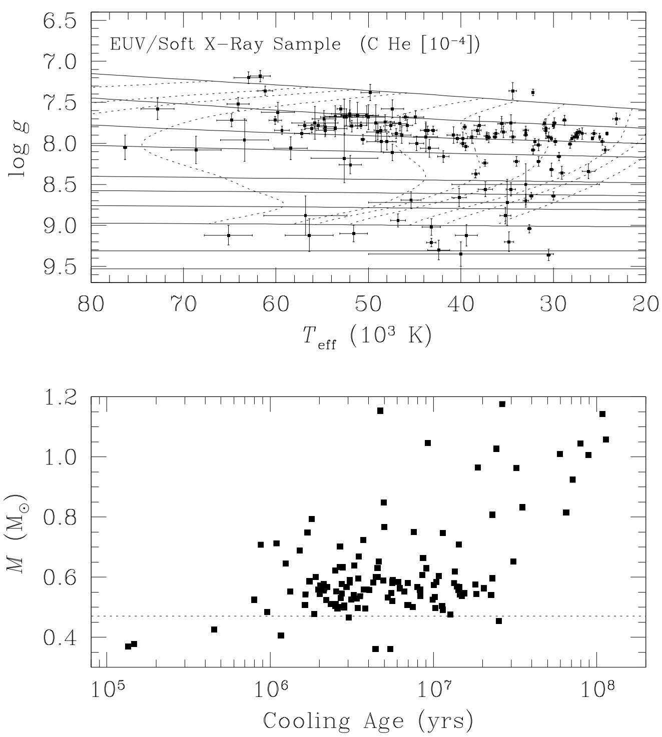

Fig. 7.—*Top*: Effective temperature and surface gravity measurements of the EUV/soft X-ray sample (141 stars) and, overlaid, Wood's (1995) evolutionary sequences at, from top to bottom, 0.4, 0.5, 0.6, 0.7, 0.9, 1.0, 1.1, and 1.2 $M_\odot$ (*full lines*), and, from left to right, 10^5, 3×10^5, 5×10^5, 10^6, 3×10^6, 5×10^6, 10^7, 3×10^7, 5×10^7, 10^8, and 3×10^8 years (*dashed lines*). Hamada & Salpeter's (1961) zero-temperature relations at 1.3 and 1.35 $M_\odot$ are also shown. *Bottom*: Mass and age measurements based on Wood's (1995) relations ($M \leq 1.2\ M_\odot$).

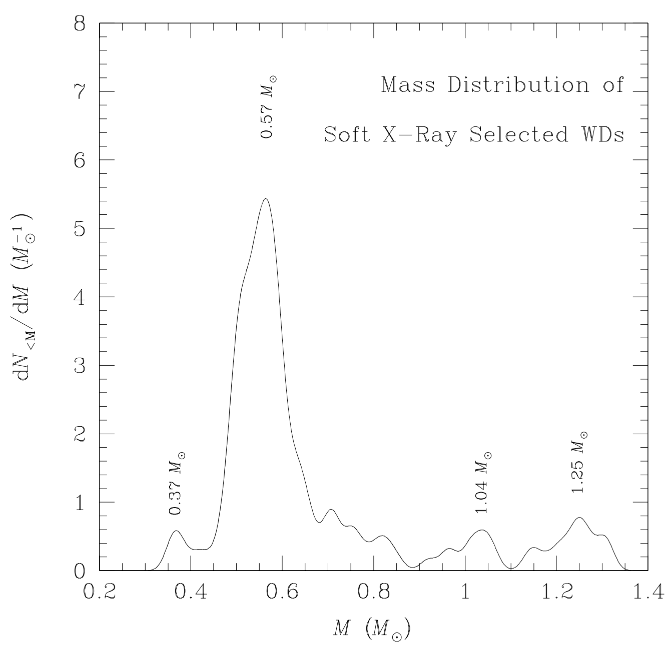

Fig. 8.—Mass distribution of the sample of 141 EUV/soft X-ray–selected white dwarfs. Sample displays population growth near 0.37, 0.57, 1.04, and 1.25 $M_\odot$. Objects with masses lower than 0.47 $M_\odot$ are helium white dwarfs, possibly formed in close binaries, while objects more massive than 1.1 $M_\odot$ may have formed via double degenerate mergers or have an ONeMg core. Most white dwarfs have a carbon/oxygen core.

low mass (0.37 $M_\odot$), average mass (0.57 $M_\odot$), high mass (1.04 $M_\odot$), and ultra-high mass (1.25 $M_\odot$). Among 15 ultramassive white dwarfs listed in Table 7, four are also magnetic, a much higher incidence than in the general white dwarf population where only four of 100 objects are identified as magnetic white dwarfs (Schmidt & Smith 1995). A higher incidence of magnetism among ultramassive white dwarfs may link these objects with early-type magnetic progenitors on the main sequence, but it may also indicate that the outcome of post-AGB evolution may be affected by stellar magnetic fields.

5. SUMMARY

I have obtained new atmospheric parameters ($T_{\rm eff}$, log g) for a sample of EUV- and soft X-ray–selected white dwarfs. Most objects are part of the list of ultrasoft X-ray sources drawn from the *ROSAT* catalog ($-1.0 \leq$ HR1 ≤ -0.9). Twelve objects were not studied previously and seven are new white dwarf identifications. Many *ROSAT* sources remain to be identified and, among those, many prospective white dwarfs.

The combined sample of EUV and soft X-ray selections now comprises 141 hot DA white dwarfs with masses ranging between 0.35 and 1.35 $M_\odot$. Some objects in the low- or high-mass range exceed predicted bounds for the formation of single white dwarfs (0.47–1.10 $M_\odot$) and may be products of close binary evolution. Radial and rotation velocity measurements rule out such scenarios in the case of the low-mass white dwarf EUVE J0512−006 and high-mass white dwarf GD 50. Our revised mass distribution now lists 15 objects with masses larger than 1.1 $M_\odot$ and, interestingly, four of these objects are magnetic. The ratio of magnetic white dwarfs in the sample of ultramassive objects largely exceeds this ratio in the general white dwarf population and may offer some clues on the origin of these objects.

I am indebted to Michelle Buxton and Dayal Wickramasinghe for their assistance with some of the observations. This work was supported in part by a NASA LTSA grant to the University of California at Berkeley, where the project was initiated, and by a QE II fellowship of the Australian Research Council.

APPENDIX A

1RXS J1016.9−4103: A NEW CATACLYSMIC VARIABLE AMONG SOFT *ROSAT* SOURCES

Red and blue DBS (SSO 2.3 m) spectra of the ultrasoft source 1RXS J1016.9−4103 show strong hydrogen Balmer and He I/He II emission lines characteristic of a magnetic CV (Fig. 9). The source was independently identified by Greiner & Schwarz (1998) and Vennes, Ferrario, & Wickramasinghe (1999b).

APPENDIX B

NEW ACTIVE GALACTIC NUCLEI AND A LATE-TYPE STAR AMONG SOFT *ROSAT* SOURCES

Table 8 lists several AGN and an active late-type star identified among the list of ultrasoft *ROSAT* sources surveyed in the present study. The spectra are shown in Figure 10 along with tentative classifications and line identifications and, for the AGNs, the measured redshifts.

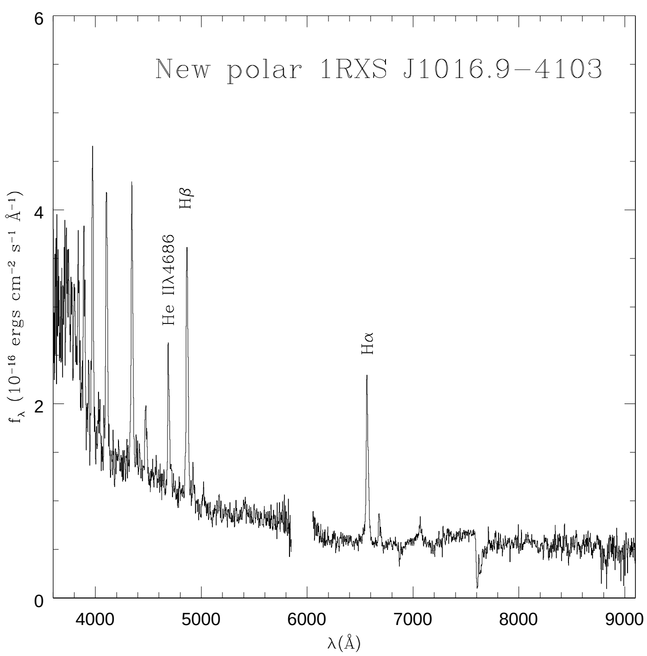

FIG. 9.—The new AM Her star 1RXS J1016.9−4103

TABLE 8

ACTIVE GALACTIC NUCLEI AND LATE-TYPE STAR

1RXS J	R.A. (2000)	Decl. (2000)	Spectral Type	z	PSPC (counts s^{-1})[a]	Hardness Ratio[a]
0007.5−4502.......	00 07 29.1	−45 02 22	QSO	0.360	0.096 ± 0.026	−1.00 ± 0.35
0039.0−1229[b]......	00 39 01.5	−12 29 12	Seyfert 1	0.282	0.070 ± 0.018	−0.95 ± 0.09
0135.3−2203.......	01 35 17.8	−22 03 54	QSO	0.380	0.114 ± 0.031	−0.92 ± 0.23
0341.1−3634.......	03 41 08.5	−36 35 16	QSO	0.347	0.117 ± 0.033	−0.95 ± 0.26
0740.2−4257.......	07 40 12.6	−42 57 52	dMe	...	0.087 ± 0.023	−0.96 ± 0.29
2109.9−4914.......	21 09 58.4	−49 14 41	Galaxy	0.0745	0.062 ± 0.017	−0.93 ± 0.19
2218.5−2911.......	22 18 29.4	−29 12 00	QSO	0.582	0.074 ± 0.022	−0.90 ± 0.18
2314.3−5258.......	23 14 19.8	−52 59 01	Seyfert 1	0.156	0.102 ± 0.025	−1.00 ± 0.10
2325.1−4551.......	23 25 05.6	−45 52 08	QSO	0.145	0.097 ± 0.028	−0.94 ± 0.31

NOTE.—Units of right ascension are hours, minutes, and seconds, and units of declination are degrees, arcminutes, and arcseconds.

[a] PSPC count rates and HR1 hardness ratio from Voges et al. 1999.

[b] = PB 8437 (Berger & Fringant 1984).

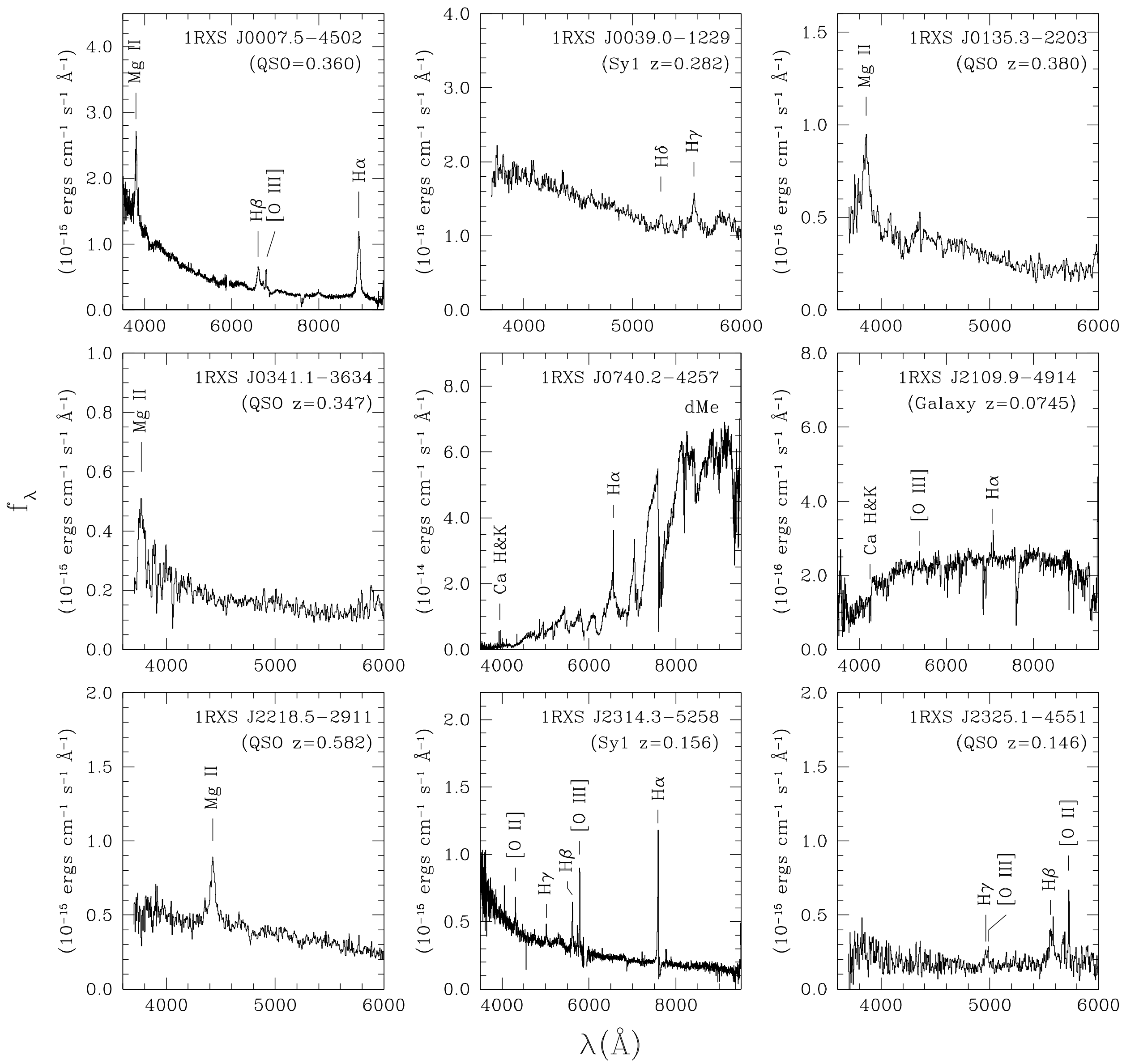

FIG. 10.—Identification spectra of nine ultrasoft X-ray sources, eight AGN, and an active late-type star. Main spectral lines are marked.

REFERENCES

Berger, J., & Fringant, A.-M. 1984, A&AS, 58, 565
Bergeron, P., Saffer, R. A., & Liebert, J. 1992, ApJ, 394, 228
Bergeron, P., Wesemael, F., Beauchamp, A., Wood, M. A., Lamontagne, R., Fontaine, G., & Liebert, J. 1994, ApJ, 432, 305
Bragaglia, A., Renzini, A., & Bergeron, P. 1995, ApJ, 443, 735
Bowyer, S., Lampton, M., Lewis, J., Wu, X., Jelinsky, P., & Malina, R. F. 1996, ApJS, 102, 129
Cheselka, M., Holberg, J. B., Watkins, R., Collins, J., & Tweedy, R. W. 1993, AJ, 106, 2365
Craig, N., Christian, D. J., Dupuis, J., Roberts, B. A. 1997, AJ, 114, 244
Dupuis, J., Vennes, S., Chayer, P., Hurwitz, M., & Bowyer, S. 1998, ApJ, 500, L45
Dupuis, J., & Vennes, S. 1997, ApJ, 475, L131
Eggen, O. J., & Greenstein, J. L. 1965, ApJ, 141, 83
Feige, J. 1958, ApJ, 128, 267
Ferrario, L., Vennes, S., & Wickramasinghe, D. T. 1998, MNRAS, 299, L1
Ferrario, L., Vennes, S., Wickramasinghe, D. T., Bailey, J. A., & Christian, D. J. 1997, MNRAS, 292, 205
Finley, D. S., Koester, D., & Basri, G. 1997, ApJ, 488, 375
Fleming, T. A., Snowden, S. L., Pfeffermann, E., Briel, U., & Greiner, J. 1996, A&A, 316, 147
Giclas, H. L., Burnham, R., & Thomas, N. G. 1965, Lowell Obs. Bull., 6, 155
———. 1975, Lowell Obs. Bull., 8, 9
Green, R. F., Schmidt, M., & Liebert, J. 1986, ApJS, 61, 305
Greenstein, J. L. 1986, AJ, 92, 867
Greiner, J., & Schwarz, R. 1998, A&A, 340, 129
Hamada, T., & Salpeter, E. E. 1961, ApJ, 134, 683
Heber, U., Napiwotzki, R., & Reid, I. N. 1997, A&A, 323, 819
Holberg, J. B., Barstow, M. A., & Sion, E. M. 1998, ApJS, 119, 207
Homeier, P., et al. 1998, A&A, 338, 563
Hubeny, I. 1988, Comput. Phys. Commun., 52, 103
Hubeny, I., & Lanz, T. 1995, ApJ, 439, 875
Iben, I., Jr., Tutukov, A. V., & Yungelson, L. R. 1997, ApJ, 475, 291
Jaidee, S., & Lynga, G. 1969, Ark. Astron., 5, 345
Kidder, K. M., Holberg, J. B, Barstow, M. A., Tweedy, R. W., & Wesemael, F. 1992, ApJ, 394, 288
Kreysing, H.-C., Brunner, H., & Staubert, R. 1995, A&AS, 114, 465
Lampton, M., Lieu, R., Schmitt, J. H. M. M., Bowyer, S., Voges, W., Lewis, J., & Wu, X. 1997, ApJS, 108, 545
Landsman, W., Simon, T., & Bergeron, P. 1993, PASP, 105, 84
Luyten, W. J., & Smith, J. A. 1958, Magnitudes and Colors of Southern White Dwarfs (Univ. of Minnesota Observ.)
Marsh, M. C., et al. 1997, MNRAS, 286, 369
Marsh, T. R., Dhillon, V. S., & Duck, S. R. 1995, MNRAS, 275, 828
Maxted, P. F. L., & Marsh, T. R. 1998, MNRAS, 296, L34
Pye, J. P., et al. 1995, MNRAS, 274, 1165
Reid, I. N., & Wegner, G. 1988, ApJ, 335, 953
Schmidt, G. D., Bergeron, P., Liebert, J., & Saffer, R. 1992, ApJ, 394, 603
Schmidt, G. D., & Smith, P. S. 1995, ApJ, 448, 305
Schwartz, R. D., Dawkins, D., Findley, D., & Chen, D. 1995, PASP, 107, 667
Segretain, L., Chabrier, G., & Mochkovitch, R. 1997, ApJ, 481, 355
Thorstensen, J. R., Charles, P. A., Margon, B., & Bowyer, S. 1978, ApJ, 223, 260
Vennes, S., Bowyer, S., & Dupuis, J. 1996, ApJ, 461, L103
Vennes, S., Ferrario, L., & Wickramasinghe, D. T. 1999a, MNRAS, 302, L49
———. 1999b, in ASP Conf. Ser. 157, Annapolis Workshop on Magnetic CVs, ed. C. Hellier & K. Mukai (San Francisco: ASP), 143
Vennes, S., Korpela, E., & Bowyer, S. 1997a, AJ, 114, 1567
Vennes, S., Thejll, P., Génova-Galvan, R., & Dupuis, J. 1997b, ApJ, 480, 714
Vennes, S., Thejll, P., & Shipman, H. L. 1991, in White Dwarfs, ed. G. Vauclair & E. Sion (Dordrecht: Kluwer), 235
Vennes, S., Thejll, P., Wickramasinghe, D. T., & Bessell, M. S. 1996, ApJ, 467, 782
Voges, W., et al. 1999, A&A, submitted
Wegner, G., & Boley, F. 1993, AJ, 105, 660
Wei, J.-Y., Cao, L., Xu, D.-W., Hu, J.-Y., & Li, Q.-B. 1997, Acta Astrophys. Sinica, 17, 107
Werner, K. 1996, ApJ, 457, L39
Wesemael, F., Auer, L. H., Van Horn, H. M., & Savedoff, M. P. 1980, ApJS, 43, 159
Wesemael, F., Henry, R. B. C., & Shipman, H. L. 1984, ApJ, 287, 868
Wolff, B., Jordan, S., & Koester, D. 1996, A&A, 307, 149
Wood, M. A. 1995, in White Dwarfs, ed. D. Koester & K. Werner (Berlin: Springer), 41